Adenosine Receptor 2A Blockade Increases the Efficacy of Anti–PD-1 through Enhanced Antitumor T-cell Responses

Paul A. Beavis[1,2], Nicole Milenkovski[1,2], Melissa A. Henderson[1,2], Liza B. John[1,2], Bertrand Allard[3], Sherene Loi[1,2], Michael H. Kershaw[1,2,4,5], John Stagg[3], and Phillip K. Darcy[1,2,4,5]

Abstract

Immunotherapy is rapidly emerging as a cancer treatment with high potential. Recent clinical trials with anti-CTLA-4 and anti–PD-1/PD-L1 antibodies (mAbs) suggest that targeting multiple immunosuppressive pathways may significantly improve patient survival. The generation of adenosine by CD73 also suppresses antitumor immune responses through the activation of A_{2A} receptors on T cells and natural killer (NK) cells. We sought to determine whether blockade of A_{2A} receptors could enhance the efficacy of anti–PD-1 mAb. The expression of CD73 by tumor cells limited the efficacy of anti–PD-1 mAb in two tumor models, and this was alleviated with concomitant treatment with an A_{2A} adenosine receptor antagonist. The blockade of PD-1 enhanced A_{2A} receptor expression on tumor-infiltrating CD8$^+$ T cells, making them more suscep-

tible to A_{2A}-mediated suppression. Thus, dual blockade of PD-1 and A_{2A} significantly enhanced the expression of IFNγ and Granzyme B by tumor-infiltrating CD8$^+$ T cells and, accordingly, increased growth inhibition of CD73$^+$ tumors and survival of mice. The results of our study indicate that CD73 expression may constitute a potential biomarker for the efficacy of anti–PD-1 mAb in patients with cancer and that the efficacy of anti–PD-1 mAb can be significantly enhanced by A_{2A} antagonists. We have therefore revealed a potentially novel biomarker for the efficacy of anti–PD-1 that warrants further investigation in patients. Because our studies used SYN-115, a drug that has already undergone phase IIb testing in Parkinson disease, our findings have immediate translational relevance for patients with cancer. *Cancer Immunol Res; 3(5); 506–17. ©2015 AACR.*

Introduction

The importance of the immune system in the control of cancers is increasingly being recognized. Tumors use multiple inhibitory pathways to suppress the immune response and thus lead to "immune escape" (1). The clinical success of therapies that block these inhibitory pathways, such as anti–PD-1 (2) and anti-CTLA-4 (3) mAbs, underlines the potential of immunotherapy to treat cancer in a more specific fashion with fewer adverse events than with conventional cancer therapies.

One mechanism of tumor-induced immune suppression is the generation of adenosine by the ectoenzyme CD73 (4). In terms of the generation of adenosine, CD73 sits downstream of the

ectoenzyme CD39 that catalyzes the degradation of ATP into AMP via the intermediate ADP. AMP then acts as a substrate for CD73, resulting in the production of immunosuppressive adenosine (4). A major enzyme for the degradation of adenosine is adenosine deaminase (ADA). ADA can be expressed on the cell surface when bound to CD26; however, CD26 expression is reduced on tumor cells (5). Thus, the tumor microenvironment contains concentrations of adenosine sufficient to inhibit antitumor T-cell responses (6).

CD73 is endogenously expressed on epithelial cells, endothelial cells, and some immune subsets, and its expression has also been observed in several cancer types, including colon cancer, melanoma, breast cancer, ovarian cancer, and leukemia (4). Notably, the expression of CD73 by tumor cells in patients with triple-negative breast cancer correlates with an increased risk of metastasis and consequently poor patient outcomes (7, 8). The drivers of CD73 expression within the tumor microenvironment include hypoxia, type I IFNs, TNFα, IL1β, prostaglandin (PG)E$_2$, and TGFβ (4). Moreover, it has been shown that certain chemotherapies, including anthracyclines, can drive CD73 expression, contributing to chemoresistance of tumor cells (8). The protumoral effect of CD73 has been validated in preclinical models showing that targeting CD73 with a mAb can reduce primary tumor growth and metastasis (9). Moreover, anti-CD73 has been shown to enhance the efficacy of chemotherapy and other immunotherapies (8, 10).

Although targeting CD73 directly has shown great therapeutic promise, there is as yet no clinical development of anti-CD73 mAbs. However, because the immunosuppressive effects of CD73 are mediated by adenosine, targeting the downstream adenosine

[1]Cancer Immunology Program, Peter MacCallum Cancer Centre, East Melbourne, Victoria, Australia. [2]Sir Peter MacCallum Department of Oncology, The University of Melbourne, Parkville, Victoria, Australia. [3]Centre de Recherche du Centre Hospitalier de l'Université de Montréal, Faculté de Pharmacie et Institut du Cancer de Montréal, Montréal, Québec, Canada. [4]Department of Pathology, University of Melbourne, Parkville, Victoria, Australia. [5]Department of Immunology, Monash University, Clayton, Victoria, Australia.

Note: Supplementary data for this article are available at Cancer Immunology Research Online (http://cancerimmunolres.aacrjournals.org/).

P.A. Beavis and N. Milenkovski contributed equally to this article.

Corresponding Authors: Phillip K. Darcy or Paul A. Beavis, Cancer Immunology Program, Peter MacCallum Cancer Centre, Locked Bag 1, A'Beckett Street, East Melbourne, VIC, 3000, Australia. Phone: 61-3-96563769; Fax: 61-3-96561411; E-mail: phil.darcy@petermac.org; paula.beavis@petermac.org

AACR

receptors has high translational potential. Activation of A$_{2A}$ and A$_{2B}$ receptors is known to suppress multiple immune cells, including the proliferation, cytokine production, and cytotoxicity of T cells (4, 11). Notably, in the context of cancer, activation of either A$_{2A}$ or A$_{2B}$ receptors has been shown to reduce antitumor immunity (6, 12, 13) and enhance the metastasis of CD73^{+} tumors (14). Moreover, antagonists targeting the A$_{2A}$ and A$_{2B}$ receptors have undergone clinical trials for other indications and have shown a good safety profile (15, 16).

In this study, we investigated whether blockade of A$_{2A}$ receptors could enhance the efficacy of anti–PD-1. Because PD-1 blockade is known to enhance T-lymphocyte function, and A$_{2A}$ expression is increased on T lymphocytes following activation (17), we hypothesized that A$_{2A}$ blockade would enhance the efficacy of anti–PD-1 by augmenting antitumor T-lymphocyte responses.

Materials and Methods

Cell lines and mice

The C57BL/6 mouse breast carcinoma cell line AT-3 was obtained from Dr. Trina Stewart (Griffith University, Nathan, QLD, Australia; ref. 18), MC38 cells were obtained from Dr. Nicole Haynes (Peter MacCallum Cancer Centre, East Melbourne, VIC, Australia), and 4T1.2 cells were obtained from Prof. Robin Anderson (Peter MacCallum Cancer Centre). Tumor cell lines were transduced to express chicken ovalbumin peptide as previously described (19, 20). These cell lines were originally obtained from the ATCC, actively passaged for less than 6 months, and were authenticated using short tandem repeat profiling. United Kingdom Co-ordinating Committee on Cancer Research (UKCCCR) guidelines for the use of cell lines in Cancer research were followed. Tumor lines were also verified to be *Mycoplasma* negative by the Victorian Infectious Diseases References Lab (Melbourne, VIC, Australia) by PCR analysis. Tumor cells were grown in DMEM supplemented with 10% FCS, GlutaMAX, and penicillin/streptomycin. For *in vivo* experiments, the indicated numbers of cells were resuspended in PBS and injected s.c. in a 100-μL volume. C57BL/6 and BALB/C wild-type (WT) mice were obtained from the Animal Resources Centre (Perth) and the Walter and Eliza Hall Institute of Medical Research (Melbourne, VIC, Australia), OT-I mice, perforin$^{-/-}$, and IFN$\gamma^{-/-}$ mice were bred in-house at the Peter MacCallum Cancer Centre, and A$_{2A}$$^{-/-}$ mice were bred at St. Vincent's Hospital (Melbourne, VIC, Australia).

Vectors and tumor cell transduction

Murine CD73 cDNA (Open Biosystems) was cloned into the pMSCV-Cherry retroviral vector. Retroviruses were made by transfection of either pMSCV-Cherry or pMSCV-Cherry-CD73 in combination with the pMD2.G envelope vector into HEK293gagpol cells using Lipofectamine 2000 (Invitrogen) as per the manufacturer's instructions. AT-3ova^{dim} and MC38ova^{dim} were transduced with pMSCV Cherry-CD73 as previously described (14).

Antibodies, agonists, and antagonists

5′-(N-Ethylcarboxamido)adenosine (NECA) and SCH58261 were purchased from Sigma. mAbs RMP1-14 (anti–PD-1 mAb), 2A3 (Isotype control). and RMT3-23 (anti-TIM-3) were purchased from BioXcell. 145-2C11 (anti-CD3 mAb) used for splenocyte

stimulation was purchased from BD Pharmingen and SIINFEKL peptide was purchased from GenScript.

OT-I cocultures

OT-I splenocytes were isolated and labeled with CFSE (1 μmol/L) as per the manufacturer's instructions (eBioscience). CFSE-labeled OT-I splenocytes were cocultured with Mitomycin-treated (5 μmol/L) MC38 ova tumor cells in the presence of SIINFEKL peptide (10 ng/mL). To indicated wells, NECA (1 μmol/L), SCH58261 (1 μmol/L), anti–PD-1 (50 μg/mL), or 2A3 isotype control were added. After 4 days, supernatants were taken for analysis of cytokine content and cells were analyzed by flow cytometry for CFSE dilution, expression of Granzyme B, and T-cell activation markers.

Analysis of adenosine receptor expression by RT-PCR

RNA was isolated from T lymphocytes using the Qiagen RNAEasy Mini Kit as per the manufacturer's instructions. To generate cDNA, mRNA was added to 1 μL of oligo dT and incubated at 65°C for 5 minutes. RNA was then added to a mixture of 4 μL 5× cDNA synthesis buffer (Promega), 2 μL 10 nmol/L dNTP mix (Promega), 1 μL 0.1 mol/L DTT (Promega), 1 μL RNase inhibitor (Promega), 1 μL Reverse Transcriptase (Promega), and 1 μL RNAase free H$_2$O. cDNA was generated at 50°C for 50 minutes and 85°C for 5 minutes before storage at −20°C until analysis of mRNA expression by qRT-PCR. Adenosine receptor expression was determined using the TaqMan Gene Expression Master Mix and primers for A$_{2A}$ and A$_{2B}$ as previously described (9). qRT-PCR for L32 and IFNγ was conducted with SYBR Green (Agilent) as per the manufacturer's instructions using the following primers: L32 forward: TTCCTGGTCCACAATGTCAAG, L32 reverse: TGTGAGCGATCTCAGCAC. IFNγ forward: GCAACAG-CAAGGCGAAAAAG and IFNγ reverse: AGCTCATTGAATGCT-TGGCG.

Analysis of tumor-infiltrating immune subsets

After euthanizing mice, tumors were excised and digested using a mix of 1 mg/mL collagenase type IV (Sigma-Aldrich) and 0.02 mg/mL DNAase (Sigma-Aldrich). After 30 minutes digestion at 37°C, cells were twice passed through a 70-μm filter. Single-cell suspensions were then prepared and analyzed by flow cytometry as previously described (14). IFNγ and Granzyme B expression was determined directly *ex vivo* using antibody clones XMG1.2 and GB11, respectively.

Determination of cAMP content of human PBMCs

PBMCs from a normal donor were isolated using Ficoll and cultured for 10 days in IMDM medium (Life Technologies) containing 30 ng/mL of OKT3 (eBioscience) and 500 U of recombinant human IL2 (Prometheus Laboratories). Activated PBMCs were resuspended in serum-free IMDM containing 500 μmol/L IBMX (Sigma) and 100 μmol/L Ro 20-1724 (Sigma) to block phosphodiesterases. SYN115 at 10 μmol/L was added to the cells 15 minutes before the addition of the A$_{2A}$ selective agonist CGS21680 (1 μmol/L). Cells were incubated with the compounds for 1 hour at 37°C and cAMP production was assayed using the cAMP Glo kit (Promega), according to the manufacturer's instructions.

Statistical analysis

Statistical differences were analyzed by the Mann–Whitney test with $P < 0.05$ considered statistically significant.

Results

Combination treatment with anti–PD-1 and A_{2A} blockade enhances the IFNγ production of $CD8^+$ T cells in vitro

To explore the link between the A_{2A} and PD-1 suppressive pathways, we first assessed the in vitro effector functions of ova-specific $CD8^+$ OT-I cells when in coculture with MC38ova^{dim} tumor cells and SIINFEKL peptide (10 nmol/L). SIINFEKL peptide was added to the cultures because robust activation of naïve OT-I cells was not observed in the absence of SIINFEKL peptide. Cocultures were performed in the presence or absence of the adenosine analogue NECA (1 μmol/L), the A_{2A} receptor antagonist SCH58261 (1 μmol/L), anti–PD-1 mAb (50 μg/mL), and/or isotype control (2A3). In the presence of NECA, the combination of anti–PD-1 and SCH58261 significantly enhanced IFNγ production ($P < 0.05$) when compared with single treatment with either agent (Fig. 1A). In the absence of exogenous NECA, neither single nor dual blockade of A_{2A} and PD-1 significantly enhanced IFNγ levels, indicating that in this assay exogenous adenosine (NECA) was required (Supplementary Fig. S1A). In contrast to the effects on IFNγ production, neither anti–PD-1 nor SCH58261 had a significant effect on proliferation as measured by CFSE dilution in this setting (Fig. 1B). The effect of A_{2A} and PD-1 blockade on the cytotoxic activity of OT-I T cells was also investigated. Although it was observed that NECA showed a trend to decrease the expression of Granzyme B by $CD8^+$ OT-I cells, and that Granzyme B expression could be significantly enhanced by the addition of either SCH58261 or anti–PD-1, there was no further increase in Granzyme B expression following dual PD-1 and A_{2A} blockade (Supplementary Fig. S1B). Furthermore, the cytotoxic activity of OT-I cells against MC38ova^{dim} tumor cells following either A_{2A} or PD-1 blockade as measured by ^{51}Cr release or CD107a staining was not modulated (Supplementary Fig. S1C and S1D). Taken together, these data indicate that combined blockade of A_{2A} and PD-1 has the capacity to enhance IFNγ production by $CD8^+$ T lymphocytes in the presence of the adenosine analogue NECA and led us to evaluate this combination therapy in vivo.

A_{2A} blockade enhances the efficacy of anti–PD-1 mAb against $CD73^+$ tumors

Because we hypothesized that adenosine may limit the efficacy of PD-1 blockade, we investigated whether the expression of CD73 by tumor cells rendered them more resistant to anti–PD-1 mAb. CD73 was ectopically expressed in the breast carcinoma cell line AT-3ova^{dim} and the colon carcinoma MC38ova^{dim} (Supplementary Fig. S2A). Although both tumor lines expressed A_{2B}, and to a lesser extent, A_1 receptors, the expression of A_{2A} was very low on AT-3 ova^{dim} tumor cells and undetectable on MC38 ova^{dim} tumor cells (Supplementary Fig. S2B). Furthermore, exposure of these tumor lines to NECA in vitro did not modulate their proliferation (Supplementary Fig. S3A) or phenotype, including expression of PD-L1 (Supplementary Fig. S3B). Taken together, this suggests that any effect of A_{2A} blockade would be mediated by modulation of the tumor microenvironment rather than tumor cells themselves.

Tumors were injected s.c. into mice and treated at day 14 once they were established (20–50 mm^2). Treatment of AT-3ova^{dim} tumors with anti–PD-1 mAb resulted in a profound and significant reduction in primary tumor growth (Fig. 2A) with a mean reduction in tumor size at day 14 after therapy of 81% (Fig. 2B). However, the efficacy of anti–PD-1 mAb against AT-3ova^{dim} $CD73^+$ tumors was significantly less than against AT-3ova^{dim} control tumors, with a mean reduction of tumor size of only 31% (Fig. 2B). These data thus show that the expression of CD73 reduced the efficacy of anti–PD-1 mAb single-agent therapy.

We hypothesized that the increased resistance of AT-3ova^{dim} $CD73^+$ tumors to anti–PD-1 monotherapy was due to A_{2A}-mediated suppression of antitumor immune responses induced by anti–PD-1 mAb. To investigate this possibility, we determined whether treatment of mice with the A_{2A} antagonist SCH58261 could enhance the therapeutic efficacy of anti–PD-1. Although A_{2A} blockade alone had no effect on the growth of AT-3ova^{dim} $CD73^+$ tumors as a single therapy (Fig. 2A), it significantly enhanced the efficacy of anti–PD-1 mAb in reducing the growth of AT-3ova^{dim} $CD73^+$ tumors (Fig. 2A). The combination of anti–PD-1 and SCH58261 (median survival, 40 days) also significantly increased the survival of mice compared with both isotype control/vehicle–
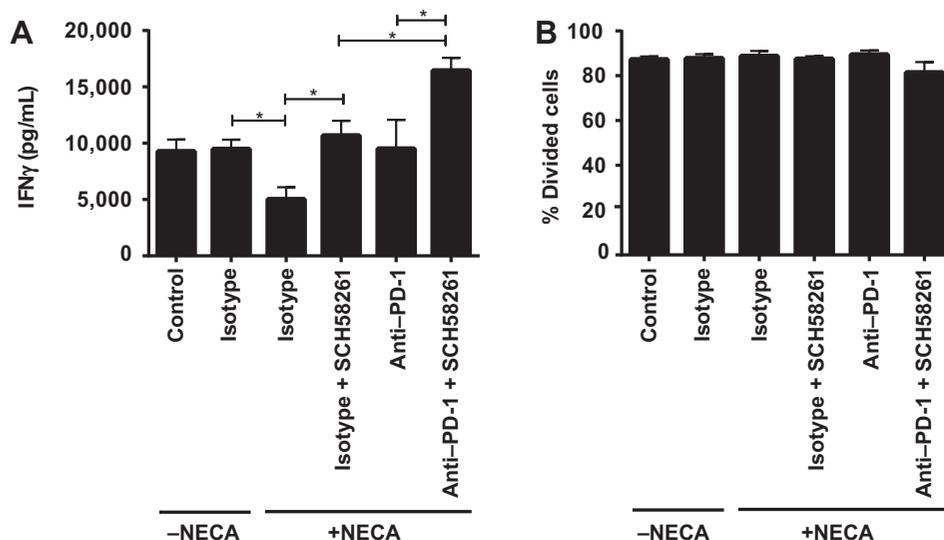

Figure 1.
Combination of A_{2A} receptor and PD-1 blockade enhances IFNγ production of OT-I splenocytes cocultured with MC38ova^{dim} tumor cells. CSFE (1 μmol/L)-labeled OT-I splenocytes were cultured with Mitomycin C (5 μmol/L)–treated MC38ova^{dim} tumor cells and SIINFEKL peptide (10 ng/mL) in the presence or absence of anti–PD-1 (50 μg/mL), SCH58261 (1 μmol/L), NECA (1 μmol/L), and/or 2A3 isotype control (50 μg/mL) for 4 days. Supernatants were collected and IFNγ concentration was determined by ELISA (A), and the percentage of $TCRβ^+CD8^+$ cells that had divided was determined by flow cytometry (B). Data are pooled from four independent experiments and presented as mean ± SEM. *, $P < 0.05$.
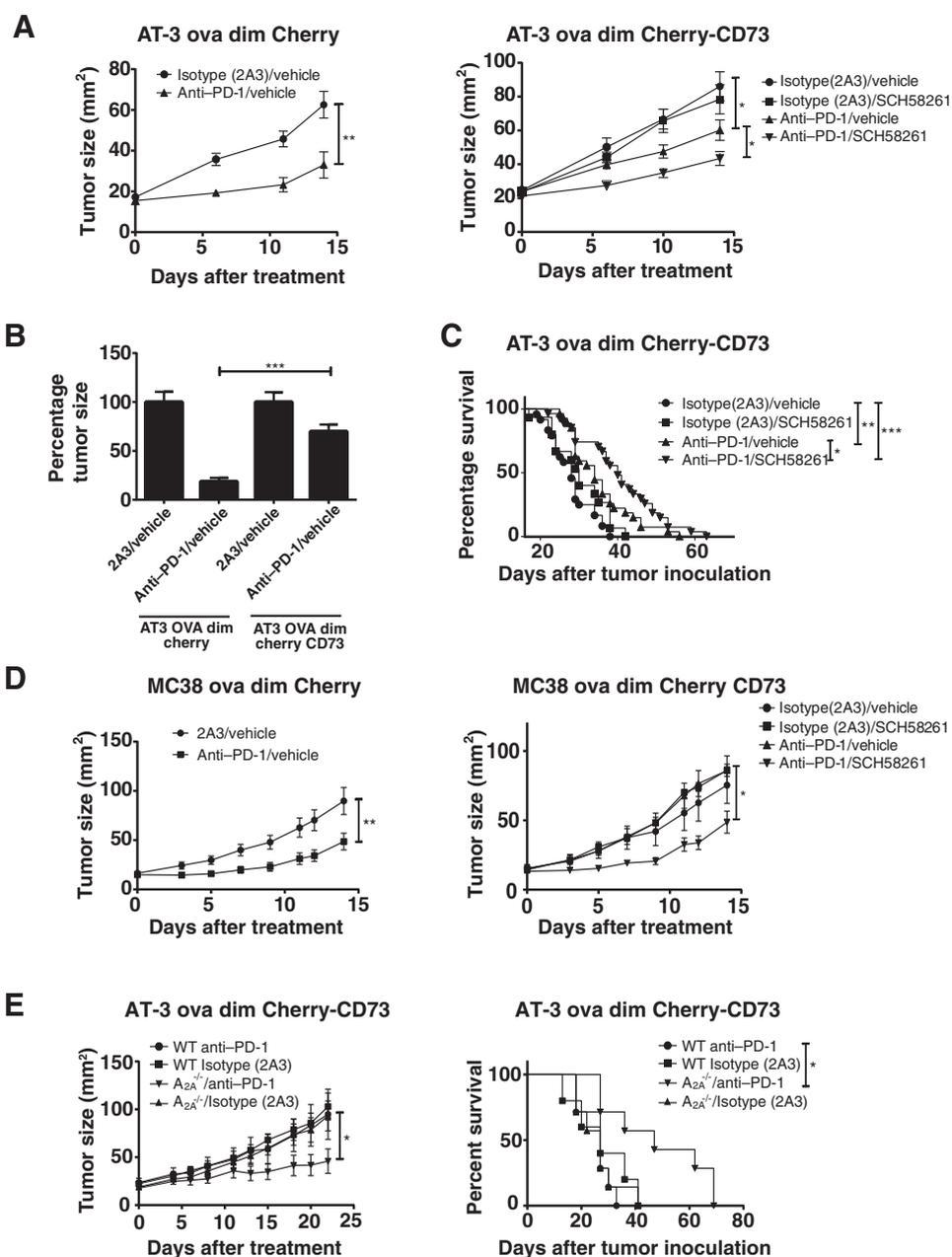
Figure 2.
A$_{2A}$ receptor blockade enhances the efficacy of anti–PD-1 against established tumors. A–E, C57BL/6 WT or (E) A$_{2A}$$^{-/-}$ mice were injected s.c. with 5×10^5 AT-3ova^{dim} Cherry (A and B), 5×10^5 AT-3ova^{dim} Cherry-CD73$^+$ (A, B, and E), 1×10^6 MC38ova^{dim} Cherry (D), or 1×10^6 MC38ova^{dim} Cherry-CD73$^+$ (D) tumor cells. A–E, mice were treated i.p. at days 14, 18, 22, and 26 with either isotype control (2A3; 200 µg/mouse) or anti–PD-1 mAb (RMP1-14, 200 µg/mouse) and where indicated SCH58261 (1 mg/kg) or vehicle control at days 14 to 29. Tumor growth and survival were monitored. A, tumor growth presented as means of 11 to 17 mice per group ± SEM. B, the mean percentage tumor size ± SEM at day 14 after therapy for 11 to 17 mice per group. C, survival of mice is shown from four pooled independent experiments ($n = 15$–27 per group). Survival was determined as when tumors grew to a size greater than 100 mm^2. D and E, data represented as the mean ± SEM of 5 to 12 mice per group for tumor growth curves and 11 to 13 mice per group for survival graph. *, $P < 0.05$; **, $P < 0.01$; ***, $P < 0.001$.

treated mice and anti–PD-1/vehicle–treated mice (median survival, 28 and 34 days, respectively; Fig. 2C). To extend these observations to another tumor model, we also compared the efficacy of anti–PD-1 mAb against established MC-38ova^{dim} and MC38ova^{dim} CD73$^+$ tumors. Similarly as with the AT-3ova^{dim} tumors, CD73 expression on MC38ova^{dim} tumor cells reduced the efficacy of anti–PD-1 mAb treatment (Fig. 2D). Furthermore, as with AT-3ova^{dim} CD73$^+$ tumors, the resistance of MC38ova^{dim} CD73$^+$ tumors to PD-1 blockade was overcome when anti–PD-1 was given in combination with SCH58261 (Fig. 2D). This result indicated that A$_{2A}$ blockade could enhance the efficacy of anti–PD-1 mAb in two distinct tumor models. To confirm that the A$_{2A}$ antagonist SCH58261 was acting through host A$_{2A}$ receptors, we determined the efficacy of anti–PD-1 mAb in WT and A$_{2A}$$^{-/-}$ mice. Indeed, anti–PD-1 mAb therapy had

significantly increased efficacy in A$_{2A}$$^{-/-}$ mice in terms of both primary tumor growth and survival (Fig. 2E), confirming the importance of host A$_{2A}$ receptors in limiting the antitumor immune response induced by PD-1 blockade.

Having clearly demonstrated that the combination of PD-1 and A$_{2A}$ blockade could treat established primary tumors, we next investigated the ability of this combination to treat the less immunogenic 4T1.2 tumor cell line. To examine this, we injected the 4T1.2 breast cancer line, which expresses CD73 endogenously, into the fourth mammary fat pad of WT mice. Mice were treated with either isotype control (2A3) or anti–PD-1 and SCH58261 or vehicle control. The combination of anti–PD-1 and SCH58261 was ineffective in reducing the primary tumor growth of 4T1.2 tumors (Fig. 3A), perhaps attributable to the low level of PD-1
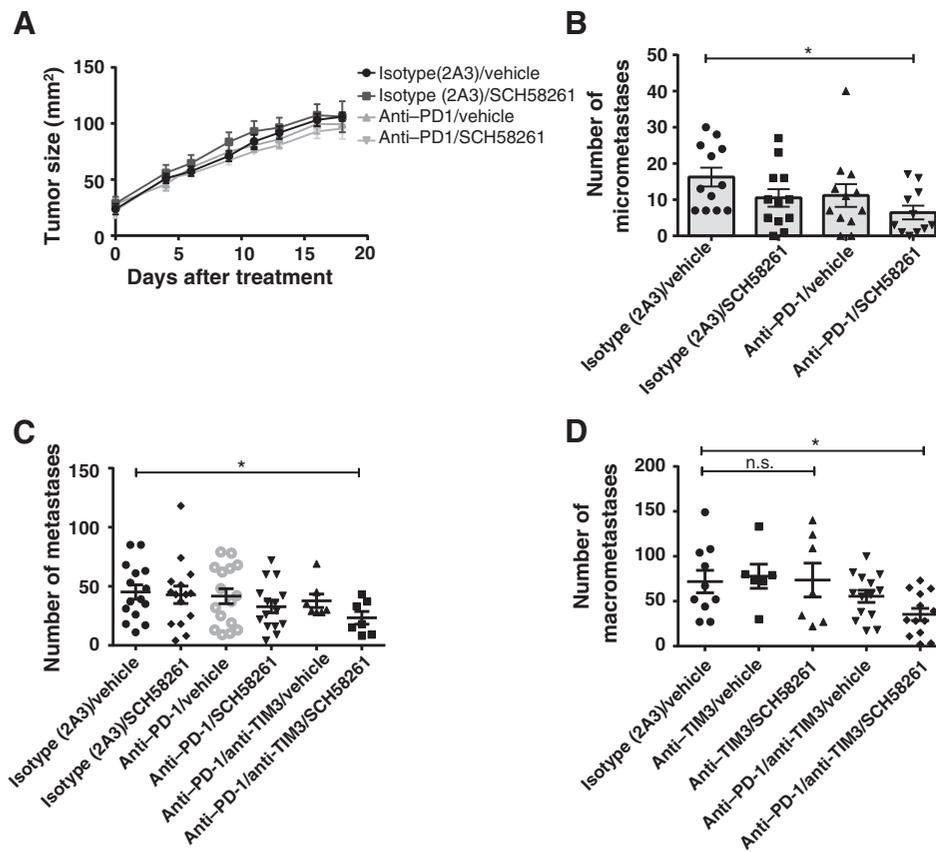
Figure 3.
A_{2A} blockade enhances the antimetastatic activity of PD-1/TIM-3 blockade. A and B, 5×10^4 4T1.2 tumor cells were injected into the fourth mammary fat pad. Seven days after injection mice were treated with either anti–PD-1, 2A3 isotype control (200 µg/ mouse), and either SCH58261 (1 mg/kg) or vehicle control. Antibody therapies were repeated 4 and 8 days after the onset of therapy and SCH58261/vehicle was given daily from day 0 to 22 after onset of therapy. A, tumor growth shown as mean ± SEM of 5 to 7 mice per group of a representative experiment. B, lung metastases were evaluated following sectioning of the lungs at day 23 after therapy (day 30 after injection) and shown as the mean ± SEM of 11 to 12 mice per group. C and D, 1×10^5 4T1.2 cells were injected i.v. into WT BALB/c mice. At days 3 and 7 after tumor injection mice were treated with 2A3 isotype control (200 µg/mouse), anti–PD-1 (200 µg/mouse), and/or anti-TIM-3 (200 µg/mouse) and at days 3 to 13 with SCH58261 (1 mg/kg) or vehicle control. Lungs were harvested at day 14 and the number of metastases enumerated. Data shown as the mean ± SEM of 7–15 mice per group. *, $P < 0.05$.

expression on T cells in this tumor model (Supplementary Fig. S4), and therefore reflecting the lower immunogenicity of this tumor line. However, the combination of anti–PD-1 and SCH58261 significantly reduced the number of spontaneous metastases in this setting (Fig. 3B). We next investigated the ability of anti–PD-1 and SCH58261 to treat established 4T1.2 lung metastases. 4T1.2 tumor cells were injected i.v., and after 3 days, mice were treated with a combination of anti–PD-1 or 2A3 isotype control mAb and SCH58261 or vehicle control. Neither anti–PD-1 nor SCH58261 was effective in reducing the number of metastases when given as a single agent (Fig. 3C). When anti–PD-1 mAb and SCH58261 were given in combination, there was a trend toward a reduction in metastases although this did not reach statistical significance.

It has previously been reported that $CD8^+$ T cells coexpress PD-1 and TIM-3 in the 4T1 breast cancer model and that anti-TIM-3 can significantly enhance the efficacy of PD-1 blockade (21). We therefore hypothesized that the inclusion of anti-TIM-3 in the treatment regimen may liberate antitumor T-cell responses sufficiently for A_{2A} blockade to become effective. Indeed, while anti–PD-1 and anti-TIM-3 showed a trend to reduce the number of tumor metastases, only the inclusion of A_{2A} blockade along with anti–PD-1 and anti-TIM-3 resulted in a significant reduction of tumor metastases (Fig. 3C). The combination of anti-TIM3 and SCH58261 had no significant effect on tumor metastases in the absence of anti–PD-1 (Fig. 3D), indicating that the blockade of multiple immunosuppressive pathways was required for the eradication of established 4T1.2 tumor metastases. Taken togeth-

er, these data highlight the ability of A_{2A} blockade to enhance the efficacy of checkpoint blockade.

PD-1 blockade enhances A_{2A} expression on $CD8^+$ tumor-infiltrating lymphocytes

Because A_{2A} expression is known to be increased following T-cell receptor (TCR) stimulation and PD-1 ligation is known to dampen TCR signaling (17, 22), we hypothesized that PD-1 blockade may increase A_{2A} expression on T lymphocytes and thus make them more susceptible to A_{2A}-mediated immunosuppression. To investigate this possibility, the expression of A_{2A} on OT-I splenocytes cocultured with (PD-L1 expressing) MC38ova^{dim} tumor cells in vitro was examined in the presence or absence of PD-1 blockade. A_{2A} expression was determined by qRT-PCR due to the lack of an antibody specific for the A_{2A} receptor suitable for flow cytometry. The expression of IFNγ was used as a positive control because it has previously been shown that PD-1 blockade enhances IFNγ production (23). As expected, PD-1 blockade significantly increased the expression of IFNγ by $CD8^+$ OT-I cells cocultured with MC38ova^{dim} tumor cells (Fig. 4A). Notably, PD-1 blockade also significantly enhanced the expression of A_{2A} receptors on $CD8^+$ OT-I cells compared with $CD8^+$ OT-I cells treated with an isotype control antibody (Fig. 4B). To investigate whether A_{2A} upregulation following PD-1 blockade also occurred in vivo, $CD8^+$ and $CD4^+$ T cells were isolated from AT-3ova^{dim} $CD73^+$ tumors following treatment of mice with either anti–PD-1 or isotype control mAb. Notably, $CD8^+$ T cells isolated from tumors of mice treated with
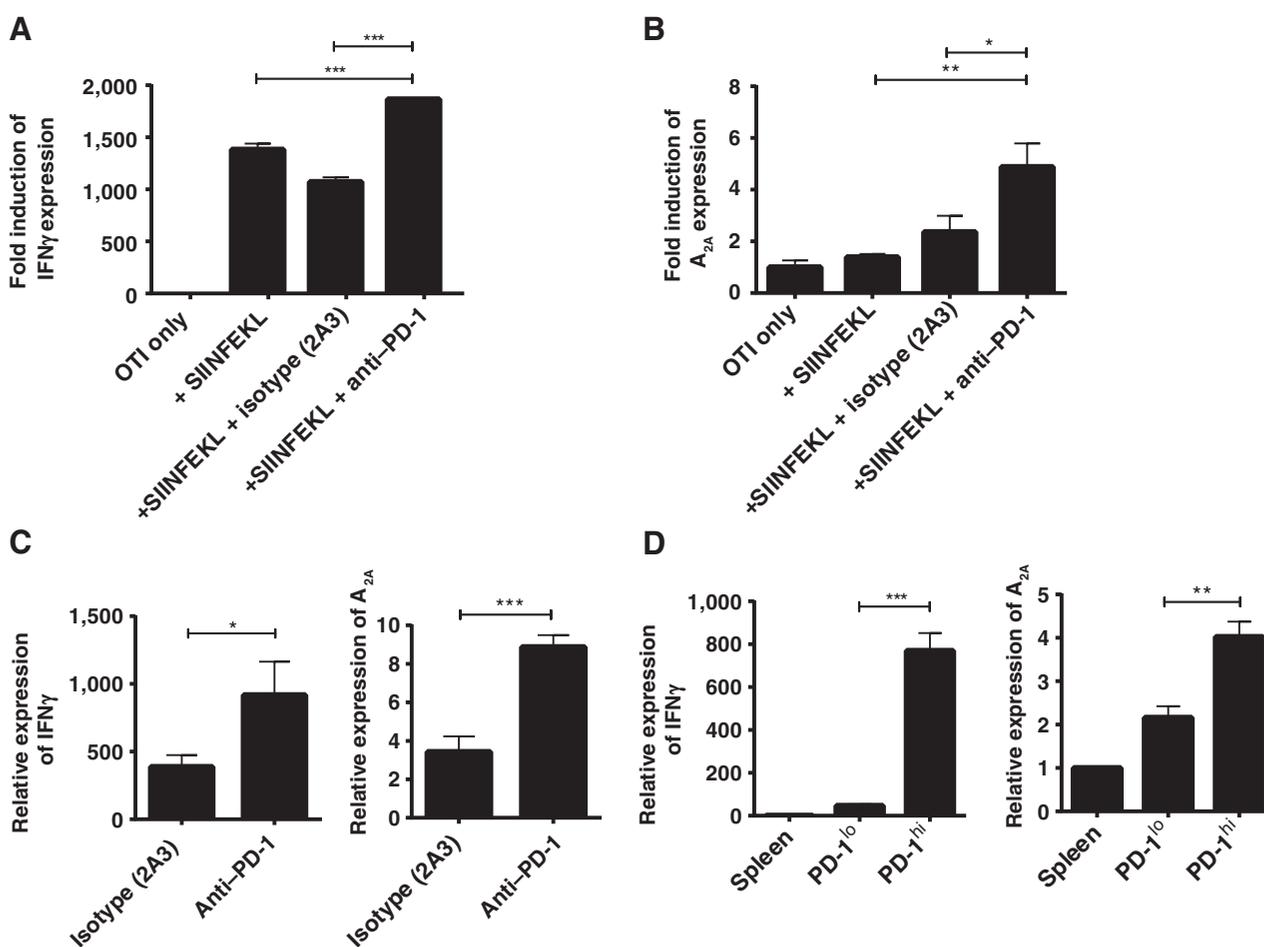
Figure 4.
PD-1 blockade enhances A$_{2A}$ receptor expression on CD8$^+$ TILs. A and B, SIINFEKL pulsed OT-I T cells were cocultured with Mitomycin C (5 µmol/L)–treated MC38ova^{dim} tumor cells in the presence or absence of SIINFEKL peptide (10 ng/mL) and either anti–PD-1 (50 µg/mL) or 2A3 isotype control (50 µg/mL). After 16 hours of coculture, cells were spun down, lysed, and analyzed for IFNγ (A) and A$_{2A}$ (B) mRNA. Data shown are triplicate values ± SD from one individual experiment representative of $n = 5$. C, TCRβ$^+$CD8$^+$ lymphocytes were FACS sorted from AT-3ova^{dim} CD73$^+$ tumors of mice 2 days after the mice were treated with either isotype control or anti–PD-1 mAb. D, TCRβ$^+$CD8$^+$PD-1^{hi} and TCRβ$^+$CD8$^+$PD-1^{low} cells were isolated from AT-3ova^{dim} CD73$^+$ tumors at day 14 after tumor inoculation. C and D, cells were isolated from 5 mice per group and then pooled and lysed. IFNγ and A$_{2A}$ expression was analyzed by qRT-PCR. Data are expressed relative to expression of naïve splenic CD8$^+$ cells and presented as mean of triplicates ± SD. *, $P < 0.05$; **, $P < 0.01$; ***, $P < 0.001$.

anti–PD-1 had significantly elevated expression of both IFNγ and the A$_{2A}$ receptor compared with those isolated from isotype control–treated mice (Fig. 4C). Furthermore, isolation of the CD8$^+$PD-1^{hi} and CD8$^+$PD-1^{low} subsets revealed that the PD-1^{hi} population had significantly elevated expression of A$_{2A}$ compared with PD-1^{low} counterparts (Fig. 4D). The increase in A$_{2A}$ expression following PD-1 blockade was restricted to CD8$^+$ T cells from within the tumor microenvironment as CD8$^+$ T cells isolated from spleens and draining lymph nodes displayed no increase in A$_{2A}$ expression (Supplementary Fig. S5A and S5B). In contrast, while CD4$^+$ T cells displayed a trend for increased expression of IFNγ following PD-1 blockade, there was no increase in A$_{2A}$ expression on these cells (Supplementary Fig. S5C). However, because the CD4$^+$ tumor-infiltrating lymphocyte (TIL) population contains a significant proportion of foxp3$^+$ cells (∼50%), the possibility that PD-1 blockade modulates A$_{2A}$ expression on either the foxp3$^-$ effector cells or foxp3$^+$ regulatory T cells cannot be discounted.

Taken together, these data indicate that PD-1 blockade enhances the expression of A$_{2A}$ receptors on tumor-infiltrating CD8$^+$ T cells and therefore increases their susceptibility to adenosine-mediated immunosuppression. These data may explain why A$_{2A}$ blockade enhances the antitumor efficacy of anti–PD-1 but has little impact on the primary growth of AT-3ova^{dim} CD73$^+$ tumor cells when administered as a single therapy (Fig. 2).

Combination of PD-1 and A$_{2A}$ blockade significantly enhances the IFNγ production of tumor-infiltrating CD8$^+$ T lymphocytes

To characterize the mechanism by which A$_{2A}$ blockade enhanced the efficacy of PD-1 mAb *in vivo*, the number and phenotype of TILs were investigated in mice bearing AT-3ova^{dim} CD73$^+$ tumors treated with either an isotype control antibody (2A3) or anti–PD-1 mAb and either SCH58261 or vehicle control. TILs were analyzed at days 1, 2, and 7 after treatment. Although the proportion of TCRβ$^+$CD8$^+$, TCRβ$^+$CD4$^+$foxp3$^-$, and TCRβ$^+$CD4$^+$foxp3$^+$ TILs was not modulated by either

anti–PD-1 alone or in combination with A_{2A} blockade (Supplementary Fig. S6A–S6C), we observed that the combination therapy significantly enhanced CD8$^+$ T-cell effector functions. Analysis of TILs at day 1 showed that treatment with anti–PD-1 significantly increased the expression of IFNγ and Granzyme B by CD8$^+$ TILs, which was not further enhanced following combination treatment with SCH58261 (Fig. 5A). However, 2 days following treatment, a significantly higher proportion of the CD8$^+$ T cells isolated from mice treated with the combination therapy were IFNγ$^+$ and Granzyme B$^+$ compared with those isolated from mice treated with anti–PD-1 mAb alone (Fig. 5A and B). The trend toward increased IFNγ production by CD8$^+$ TILs in the combination group extended to day 7 after therapy with only the combination therapy giving a significantly enhanced proportion of IFNγ$^+$ CD8$^+$ TILs compared

with isotype control/vehicle–treated mice (Supplementary Fig. S7). Thus, although the initial response to anti–PD-1 mAb was not affected by A_{2A} blockade, the induced CD8$^+$ T-cell response was maintained by the A_{2A} antagonist SCH58261. In contrast, no increased expression of IFNγ was seen on CD4$^+$ TILs following either anti–PD-1 mAb single-agent therapy or anti–PD-1 mAb/SCH58261 combination therapy at either time point (Supplementary Fig. S8A). We also investigated the effect of A_{2A} blockade on the expression of PD-1 on TILs. SCH58261 had no significant effect on PD-1 expression either in combination with PD-1 blockade (Supplementary Fig. S6) or on its own (Supplementary Fig. S9A). Moreover, A_{2A} blockade did not affect the expression of PD-L1 on tumor cells (Supplementary Fig. S9B), further suggesting that the efficacy of PD-1/A_{2A} blockade was due to enhanced T-cell effector function.
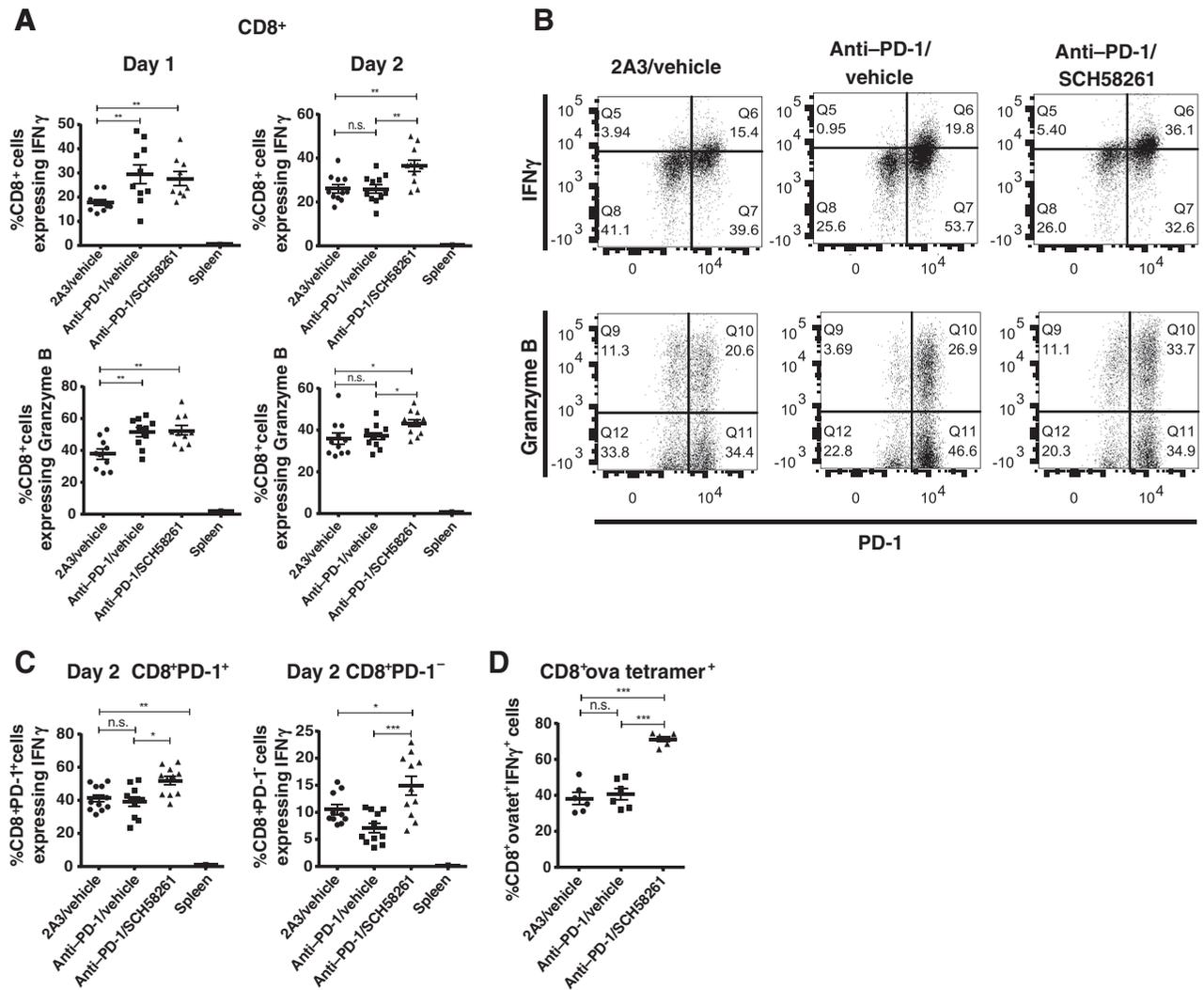

Figure 5.
Combined A_{2A} receptor and PD-1 blockade significantly enhances the IFNγ production of CD8$^+$ TILs. C57BL/6 WT mice were injected s.c. with 5×10^5 AT-3ova^{dim} CD73$^+$ tumor cells. After 14 days, mice were treated i.p. with either an isotype control antibody (2A3, 200 μg/mouse) or anti–PD-1 mAb (RMP1–14, 200 μg/mouse) and either SCH58261 (1 mg/kg) or vehicle control at days 0 and 1 after anti–PD-1 mAb therapy. TILs were isolated from AT-3ova^{dim} CD73$^+$ tumors 1 to 2 days after treatment and analyzed for expression of IFNγ, Granzyme B, PD-1, and ova tetramer reactivity by flow cytometry. The expression of IFNγ and Granzyme B by splenic TCRβ$^+$CD8$^+$ cells is shown as a comparator. A, data shown for a minimum of 10 mice per group pooled from two separate experiments and shown as mean ± SEM. B, representative flow cytometry analysis from one mouse per group 2 days after treatment. C and D, data represented as mean ± SEM of $n = 5$–11. *, $P < 0.05$; **, $P < 0.01$; ***, $P < 0.001$.

To further investigate the CD8$^+$ T-cell populations modulated by the combination therapy, we analyzed IFNγ production and Granzyme B expression of the CD8$^+$PD-1^{hi} cells and CD8$^+$PD-1^{low} cells. Interestingly, dual anti–PD-1 mAb and SCH58261 treatment significantly increased the expression of IFNγ in both the CD8$^+$PD-1^{hi} and CD8$^+$PD-1^{low} subsets compared with anti–PD-1 alone (Fig. 5C). In contrast, Granzyme B expression was more selectively modulated by the combination therapy in the CD8$^+$PD-1^{hi} population (Supplementary Fig. S8B). As with the analysis of the global CD8$^+$ TIL population (Fig. 5A), the increase in IFNγ production by the CD8$^+$PD-1^{hi} cells following combination therapy was seen at day 2 (Fig. 5C) but not at day 1 (Supplementary Fig. S8C), indicating that A$_{2A}$ blockade maintained the activation induced by anti–PD-1 mAb.

We next investigated whether the antigen-specific CD8$^+$ T-cell population was modulated by anti–PD-1 mAb/SCH58261 treatment. Although PD-1 blockade enhanced the proportion of CD8$^+$ TILs that were ova tetramer specific, the addition of the A$_{2A}$ antagonist did not further enhance this effect (Supplementary Fig. S8D). Notably, however, a significantly higher proportion of these ova tetramer$^+$ TILs expressed IFNγ when isolated from anti–PD-1/SCH58261-treated mice compared with mice treated with anti–PD-1 mAb alone (Fig. 5D). No increase in IFNγ or Granzyme B was observed within CD8$^+$ TILs in mice treated with SCH58261 in the absence of anti–PD-1, confirming that the combination of PD-1 and A$_{2A}$ blockade was required for this effect (Supplementary Fig. S9C and S9D). Taken together, these data indicate that the enhanced efficacy of anti–PD-1 mAb/SCH58261 treatment was due to enhanced effector function of TILs as opposed to increased proliferation and/or recruitment. To determine the functional importance of increased IFNγ secretion and Granzyme B expression in terms of the antitumor immune response induced by the combination of anti–PD-1 mAb and SCH58261, the efficacy of this combination therapy was determined in IFN$\gamma^{-/-}$ and perforin$^{-/-}$ mice. The effectiveness of anti–PD-1 mAb/SCH58261 was completely abrogated in IFN$\gamma^{-/-}$ mice but not perforin$^{-/-}$ mice, indicating that the increased IFNγ production induced by the combination of SCH58261 and anti–PD-1 mAb was critical for its improved efficacy (Fig. 6).

Enhancement of anti–PD-1 function with the clinical trial drug SYN115

To enhance the translational relevance of our study, we also assessed the potential of SYN115, an A$_{2A}$ antagonist that has undergone phase IIb clinical trials (16), to enhance anti–PD-1 function. Established AT-3ova^{dim} CD73$^+$ tumors were treated with an isotype control or anti–PD-1 mAb in combination with either SCH58261, SYN115, or vehicle. We observed that SYN115 had no single-agent activity, but significantly enhanced the antitumor efficacy of anti–PD-1 mAb (Fig. 7A) to a similar extent as SCH58261 (Fig. 7B). SYN115 was also able to significantly inhibit the increased cAMP concentrations mediated by the specific A$_{2A}$ agonist CGS21680 on activated human PBMCs (Fig. 7C). Thus, an A$_{2A}$ antagonist known to be safe and well tolerated in patients can enhance the antitumor efficacy of anti–PD-1 mAb, underlining the potential of this combination therapy to be translated into the clinic.

Discussion

It is increasingly recognized that immunotherapy is an effective strategy in several cancer types. In particular, recent results from clinical trials indicate that PD-1 blockade is a powerful emerging immunotherapeutic strategy (2). However, the success of anti–PD-1 therapy is limited to a subset of patients and thus further work is required to enhance the therapeutic benefit of anti–PD-1 and improve our understanding of where PD-1 blockade is most likely to provide patient benefit. For example, the success rate of PD-1 blockade can be improved if patients are selected on the basis of their tumors expressing the PD-1 ligand PD-L1 (2, 24).

The identification of additional biomarkers that are predicative of the response to anti–PD-1 mAb would be an important advance in our understanding, especially considering the prohibitive expense of immunotherapy. We have previously reported that CD73 is a negative prognostic marker for triple-negative breast cancer and predictive of a poor objective response to anthracycline therapy (8). Herein, we describe data indicating that the expression of CD73 by tumor cells also significantly reduces the efficacy of anti–PD-1 and that this can be overcome with blockade of A$_{2A}$ receptors. We focused on the ability of A$_{2A}$ blockade to enhance the efficacy of anti–PD-1 mAb because A$_{2A}$ is upregulated on T cells following activation (17) and has an affinity for adenosine approximately 1,000-fold greater than that of A$_{2B}$. However, the blockade of other adenosine receptors such as A$_{2B}$ may also enhance the therapeutic efficacy of anti–PD-1 either directly or through indirect mechanisms such as the modulation of dendritic cells (12) or myeloid-derived suppressor cells (25).

Because we have shown that the CD73:A$_{2A}$ pathway can limit the efficacy of anti–PD-1 therapy, it would be interesting to
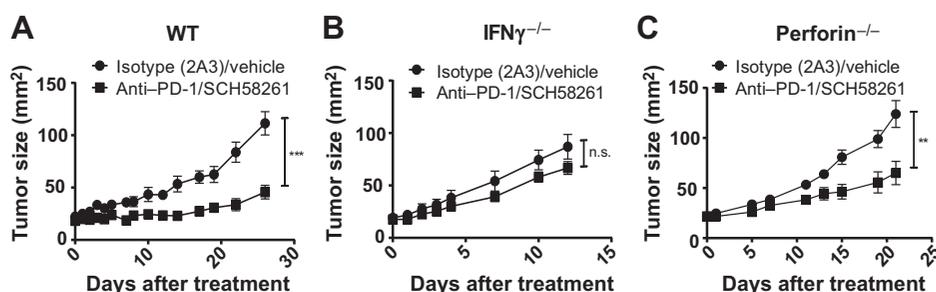

Figure 6.
Combined A$_{2A}$ receptor and PD-1 blockade is not effective in IFN$\gamma^{-/-}$ mice. AT-3ova^{dim} CD73$^+$ tumor cells (5 × 10^5) were injected into C57BL/6 WT (A), IFN$\gamma^{-/-}$ (B), or perforin$^{-/-}$ (C) mice. Mice were treated i.p. at days 14, 18, 22, and 26 with either isotype control (2A3; 200 µg/mouse) or anti–PD-1 mAb (RMP1-14, 200 µg/mouse) and where indicated SCH58261 (1 mg/kg) or vehicle control at days 14 to 29. Data represented as mean ± SEM of n = 6-7. n.s., not statistically significant; **, P < 0.01; ***, P < 0.001.
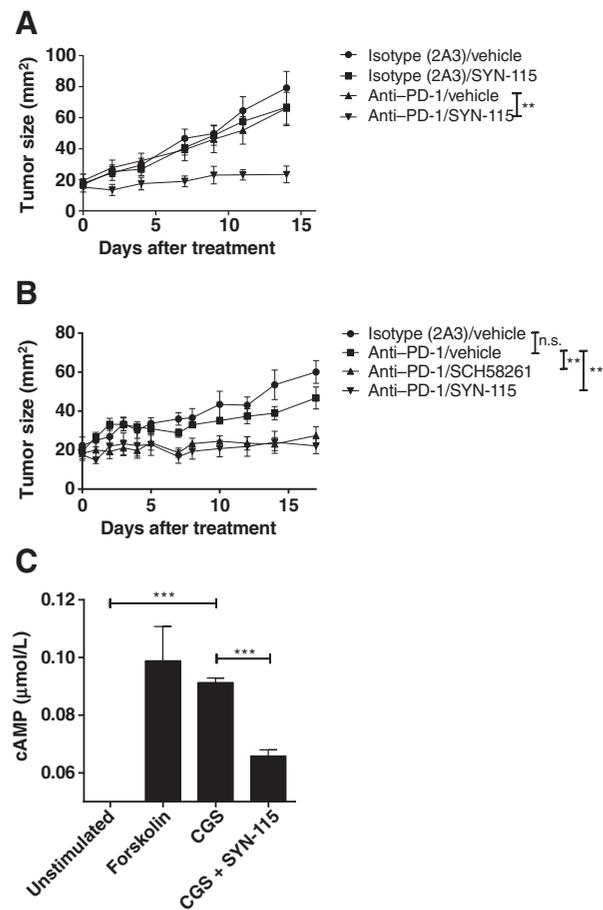

Downloaded from http://aacrjournals.org/cancerimmunolres/article-pdf/3/5/506/2347526/506.pdf by guest on 23 May 2022

Figure 7.
The clinical trial A$_{2A}$ receptor antagonist SYN115 enhances the efficacy of anti–PD-1 against established AT-3ova^{dim} CD73$^+$ tumors. A and B, C57BL/6 WT mice were injected s.c. with 5×10^5 AT-3ova^{dim} CD73$^+$ tumor cells. Mice were treated i.p. at days 14, 18, 22, and 26 with either an isotype control antibody (2A3, 200 µg/mouse) or anti–PD-1 mAb (RMP1-14, 200 µg/mouse) and either SCH58261 (1 mg/kg), SYN115 (1 mg/kg) or vehicle control at days 14 to 29. Data shown are mean ± SEM of 5 mice per group for a representative experiment of $n = 3$. C, human PBMCs were activated with OKT3 and IL2 for 10 days. Cells (3×10^5) were then treated with either forskolin (250 µmol/L), CGS21680 (1 µmol/L), or SYN115 (10 µmol/L). ***, $P < 0.001$; **, $P < 0.01$; n.s., not statistically significant.

evaluate whether CD73 is a biomarker for the clinical responses to anti–PD-1 mAb therapy in patients. Recently, a phase I study reported that combining CTLA-4 and PD-1 blockade may improve the efficacy of either treatment alone (26). This is further supported by a large body of preclinical data that combining PD-1 blockade with other immunotherapies, including anti-CTLA-4 (27–30), anti-TIM-3 (21), anti-OX40 (31), anti-CD73 (10) anti-CD137 (32), anti-GITR (33), cancer vaccines (29), radiotherapy (34), chemotherapy (32), and adoptive cellular therapy (35), can significantly enhance antitumor immune responses. The results of a recent study suggested that PD-1 blockade could enhance the antimetastatic activity of A$_{2A}$ blockade through enhanced natural killer (NK) cell responses (36). Our data indicate that A$_{2A}$ blockade also enhances the efficacy of anti–PD-1 mAb in a primary tumor setting and warrant further investigation as a combination therapy. In contrast with these authors, how-

ever, we found that the enhanced efficacy of PD-1/A$_{2A}$ dual blockade was due to enhanced CD8$^+$ T-cell function and found little expression of PD-1 on NK cells in the 4T1.2 tumor model. If both mechanisms are valid, this suggests that enhanced NK cell function is an indirect consequence of PD-1 blockade. Furthermore, we also show that A$_{2A}$ blockade was able to enhance the efficacy of anti–PD-1 against established 4T1.2 lung metastases only when given in combination with anti-TIM-3. These data highlight that treatment of more established metastatic disease may require blockade of multiple inhibitory pathways.

The efficacy of A$_{2A}$ antagonists when given in combination with anti–PD-1 is likely related to the fact that PD-1 blockade enhances the expression of A$_{2A}$ receptors on tumor antigen–specific CD8$^+$ TILs, therefore making them more susceptible to adenosine-mediated immunosuppression. The mechanism by which PD-1 blockade enhances A$_{2A}$ expression is not known. However, A$_{2A}$ expression is known to be increased in T lymphocytes following TCR activation (17) and PD-1 has been shown to suppress Ca^{2+} ERK responses immediately downstream of the TCR (22). Therefore, it seems likely that the mechanism by which PD-1 blockade increases A$_{2A}$ expression is a direct consequence of enhanced TCR signaling, at least in part. Indeed, this hypothesis is supported by the fact that upregulation of A$_{2A}$ on antitumor CD8$^+$ T cells was seen both in vitro and in vivo following PD-1 blockade. Furthermore, because our data indicate that A$_{2A}$ is more highly expressed on PD-1$^+$ cells, the blockade of PD-1 may lead to the enrichment of the PD-1$^+$ subset and consequently increase the proportion of CD8$^+$ T cells susceptible to A$_{2A}$-mediated suppression. In this study, we did not observe that A$_{2A}$ blockade significantly modulated PD-1 expression on CD8$^+$ or CD4$^+$ T cells. Although our observation appears to contrast with the observations of Cekic and Linden (37), the difference may be that in our study A$_{2A}$ blockade was conducted in established tumors in which memory T cells have already differentiated or because the pharmacologic antagonist SCH58261 does not mediate full A$_{2A}$ blockade. Therefore, the timing and magnitude of A$_{2A}$ blockade may be crucial to the therapeutic outcome.

It has been proposed that the additional benefit of combined CTLA-4 and PD-1 blockade is attributable to the fact that PD-1 and CTLA-4 inhibit T-cell activation via distinct signaling pathways (38, 39). This is also the case for A$_{2A}$ blockade. Although PD-1 signaling decreases the phosphorylation of proximal TCR signaling proteins, such as CD3ξ, ZAP70, PI3K, and PKCθ, via the recruitment of SHP-1 and SHP-2 (38–41), A$_{2A}$ activation acts to suppress T cells via enhanced cAMP concentrations. This process results in the activation of PKA, which consequently inhibits the activity of NFAT (42, 43), NFκB (44), and MAPK (45). Therefore, there is a precedent to evaluate the potential benefit of dual A$_{2A}$ and PD-1 blockade in the clinic, especially among the cohort of patients who do not respond well to anti–PD-1 alone.

Although A$_{2A}$ blockade did not enhance either the proportion of CD8$^+$ T cells or the frequency of antigen-specific CD8$^+$ cells, our findings indicate that the combination of PD-1 and A$_{2A}$ blockade was able to significantly increase the production of IFNγ by antitumor T cells both in vitro and in vivo. Interestingly, while anti–PD-1 mAb single therapy was able to induce a similar upregulation of IFNγ on CD8$^+$ cells 24 hours after treatment compared with combination therapy, the combination of A$_{2A}$

blockade and PD-1 blockade resulted in significantly more IFNγ$^+$ cells 48 hours after treatment. This indicates that A$_{2A}$ blockade sustains the anti–PD-1 response and is likely due to the upregulation of A$_{2A}$ receptors on CD8$^+$ TILs following PD-1 blockade. Although the increase in IFNγ production was most marked in the antigen-specific CD8$^+$PD-1^{hi} population, we also observed an increased production of IFNγ in the CD8$^+$PD-1^{low} subset following combination therapy. The reason for this is not known but it is possible that the PD-1^{low} subset is indirectly affected because of proinflammatory cytokines secreted by the PD-1^{hi} cells, leading to increased activation of the PD-1^{low} cells themselves, as well as activation of other immune subsets, including APCs. We observed no increased expression of IFNγ by CD4$^+$ T cells following PD-1 blockade despite expression of PD-1 by these TILs. This may be explained by the fact that CD4$^+$ T cells are less sensitive to PD-1–mediated inhibition than CD8$^+$ T cells (46). However, it should be noted that one caveat with these experiments is that we did not distinguish between foxp3$^-$ and foxp3$^+$ cells, which may have skewed our interpretation of these results. Nevertheless, the increased efficacy of PD-1 and A$_{2A}$ blockade, compared with anti–PD-1 mAb alone, seems largely attributable to an increased IFNγ response from CD8$^+$PD-1$^+$ tumor antigen–specific TILs. Indeed, the combination therapy of PD-1/A$_{2A}$ blockade was ineffective in IFNγ$^{-/-}$ mice. These results are consistent with observations by other groups that blockade of other checkpoint inhibitors, such as CTLA-4 or TIM-3 (21, 27, 47), can enhance IFNγ production by CD8$^+$ TILs following anti–PD-1 mAb treatment.

Although our results suggest that the enhanced therapeutic activity of dual PD-1 and A$_{2A}$ blockade is related to enhanced IFNγ responses, we also observed that A$_{2A}$ blockade enhanced the expression of Granzyme B in CD8$^+$ TILs when given in combination with anti–PD-1. Whether this translates to enhanced cytotoxic function is not clear, however, because we observed no evidence of PD-1 or A$_{2A}$ blockade enhancing cytotoxic function of CD8$^+$ T cells *in vitro*. This discrepancy may be explained by the activation status of the CD8$^+$ T cells used in our *in vitro* assays because the cells used for typical *in vitro* "killing assays" are preactivated with high doses of IL2. It is known that activation of CD8$^+$ T cells with IL2 can overcome the suppression mediated by PD-1 (46). Other groups have previously observed enhanced CTL function following PD-1 blockade (48, 49) using different experimental systems. Our experiments with perforin$^{-/-}$ mice show that enhanced cytolytic function is not critical for the efficacy of the combination therapy. Notably, however, although the efficacy of the combination therapy was not abolished in perforin$^{-/-}$ mice, the extent of tumor control appeared to be somewhat reduced in these mice when compared with WT controls. Thus, it remains possible that the efficacy of combination therapy *in vivo* may also be attributable in part to enhanced cytotoxic T-cell function.

In this study, we provide evidence that CD73 expression is a negative prognostic marker with regard to the therapeutic efficacy of PD-1 blockade and that A$_{2A}$ antagonists may be a viable option to improve the clinical efficacy of anti–PD-1 mAb therapy. Interestingly, it has recently been reported that A$_{2A}$ blockade can also enhance the function of CTLA-4 mAb in a murine melanoma model (50). This suggests that A$_{2A}$ blockade may be able to enhance the clinical efficacy of other checkpoint inhibitors. Several A$_{2A}$ antagonists have undergone clinical trials for Parkinson disease, including istradefylline (KW-6002-phase III), preladenant (SCH-420814 phase II; ref. 15), and SYN-115 (phase IIb; ref. 16), the compound used in our studies. These drugs have thus far been found to be safe and well tolerated, indicating that they could be readily applied to patients with cancer. Therefore, our work using A$_{2A}$ antagonists to block the CD73 pathway carries strong clinical relevance given that no anti-CD73 mAbs are in clinical development. Our studies have revealed a previously unreported function of SYN-115 in enhancing antitumor immunity, underlining the fact that the combination of PD-1 and A$_{2A}$ blockade has immediate translational potential.

Disclosure of Potential Conflicts of Interest

Authors' Contributions

Conception and design: P.A. Beavis, J. Stagg, P.K. Darcy
Development of methodology: P.A. Beavis, N. Milenkovski, P.K. Darcy
Acquisition of data (provided animals, acquired and managed patients, provided facilities, etc.): P.A. Beavis, N. Milenkovski, M.A. Henderson, L.B. John, B. Allard, P.K. Darcy
Analysis and interpretation of data (e.g., statistical analysis, biostatistics, computational analysis): P.A. Beavis, N. Milenkovski, S. Loi, M.H. Kershaw, P.K. Darcy
Writing, review, and/or revision of the manuscript: P.A. Beavis, N. Milenkovski, M.A. Henderson, B. Allard, S. Loi, J. Stagg, P.K. Darcy
Administrative, technical, or material support (i.e., reporting or organizing data, constructing databases): P.A. Beavis, N. Milenkovski, P.K. Darcy
Study supervision: P.A. Beavis, M.H. Kershaw, J. Stagg, P.K. Darcy

Acknowledgments

Grant Support

References

1. Stewart TJ, Smyth MJ. Improving cancer immunotherapy by targeting tumor-induced immune suppression. Cancer Metastasis Rev 2011;30: 125–40.

2. Topalian SL, Hodi FS, Brahmer JR, Gettinger SN, Smith DC, McDermott DF, et al. Safety, activity, and immune correlates of anti-PD-1 antibody in cancer. N Engl J Med 2012;366:2443–54.

3. Robert C, Thomas L, Bondarenko I, O'Day S, Weber J, Garbe C, et al. Ipilimumab plus dacarbazine for previously untreated metastatic melanoma. N Engl J Med 2011;364:2517–26.

4. Beavis PA, Stagg J, Darcy PK, Smyth MJ. CD73: a potent suppressor of antitumor immune responses. Trends Immunol 2012; 33:231–7.

5. Linden J. Adenosine metabolism and cancer. Focus on "Adenosine down-regulates DPPIV on HT-29 colon cancer cells by stimulating protein tyrosine phosphatases and reducing ERK1/2 activity via a novel pathway". Am J Physiol Cell Physiol 2006;291:C405–6.

6. Ohta A, Gorelik E, Prasad SJ, Ronchese F, Lukashev D, Wong MK, et al. A2A adenosine receptor protects tumors from antitumor T cells. Proc Natl Acad Sci U S A 2006;103:13132–7.

7. Leth-Larsen R, Lund R, Hansen HV, Laenkholm AV, Tarin D, Jensen ON, et al. Metastasis-related plasma membrane proteins of human breast cancer cells identified by comparative quantitative mass spectrometry. Mol Cell Proteomics 2009;8:1436–49.

8. Loi S, Pommey S, Haibe-Kains B, Beavis PA, Darcy PK, Smyth MJ, et al. CD73 promotes anthracycline resistance and poor prognosis in triple negative breast cancer. Proc Natl Acad Sci U S A 2013;110: 11091–6.

9. Stagg J, Divisekera U, McLaughlin N, Sharkey J, Pommey S, Denoyer D, et al. Anti-CD73 antibody therapy inhibits breast tumor growth and metastasis. Proc Natl Acad Sci U S A 2010;107:1547–52.

10. Allard B, Pommey S, Smyth MJ, Stagg J. Targeting CD73 enhances the antitumor activity of anti-PD-1 and anti-CTLA-4 mAbs. Clin Cancer Res 2013;19:5626–35.

11. Stagg J, Smyth MJ. Extracellular adenosine triphosphate and adenosine in cancer. Oncogene 2010;29:5346–58.

12. Cekic C, Sag D, Li Y, Theodorescu D, Strieter RM, Linden J. Adenosine A2B Receptor Blockade Slows Growth of Bladder and Breast Tumors. J Immunol 2012;188:198–205.

13. Jin D, Fan J, Wang L, Thompson LF, Liu A, Daniel BJ, et al. CD73 on tumor cells impairs antitumor T-cell responses: a novel mechanism of tumor-induced immune suppression. Cancer Res 2010;70:2245–55.

14. Beavis PA, Divisekera U, Paget C, Chow MT, John LB, Devaud C, et al. Blockade of A2A receptors potently suppresses the metastasis of CD73$^+$ tumors. Proc Natl Acad Sci U S A 2013;110:14711–6.

15. Park A, Stacy M. Istradefylline for the treatment of Parkinson's disease. Expert Opin Pharmacother 2012;13:111–4.

16. Black KJ, Koller JM, Campbell MC, Gusnard DA, Bandak SI. Quantification of indirect pathway inhibition by the adenosine A2a antagonist SYN115 in Parkinson disease. J Neurosci 2010;30:16284–92.

17. Lappas CM, Rieger JM, Linden J. A2A adenosine receptor induction inhibits IFN-gamma production in murine CD4$^+$ T cells. J Immunol 2005;174: 1073–80.

18. Stewart TJ, Abrams SI. Altered immune function during long-term host-tumor interactions can be modulated to retard autochthonous neoplastic growth. J Immunol 2007;179:2851–9.

19. Mattarollo SR, Loi S, Duret H, Ma Y, Zitvogel L, Smyth MJ. Pivotal role of innate and adaptive immunity in anthracycline chemotherapy of established tumors. Cancer Res 2011;71:4809–20.

20. Gilfillan S, Chan CJ, Cella M, Haynes NM, Rapaport AS, Boles KS, et al. DNAM-1 promotes activation of cytotoxic lymphocytes by nonprofessional antigen-presenting cells and tumors. J Exp Med 2008;205: 2965–73.

21. Sakuishi K, Apetoh L, Sullivan JM, Blazar BR, Kuchroo VK, Anderson AC. Targeting Tim-3 and PD-1 pathways to reverse T cell exhaustion and restore anti-tumor immunity. J Exp Med 2010;207:2187–94.

22. Wang SF, Fouquet S, Chapon M, Salmon H, Regnier F, Labroquere K, et al. Early T cell signalling is reversibly altered in PD-1$^+$ T lymphocytes infiltrating human tumors. PLoS ONE 2011;6:e17621.

23. Fourcade J, Kudela P, Sun Z, Shen H, Land SR, Lenzner D, et al. PD-1 is a regulator of NY-ESO-1–specific CD8$^+$ T cell expansion in melanoma patients. J Immunol 2009;182:5240–9.

24. Taube JM, Klein AP, Brahmer JR, Xu H, Pan X, Kim JH, et al. Association of PD-1, PD-1 ligands, and other features of the tumor immune microenvironment with response to anti-PD-1 therapy. Clin Cancer Res 2014; 20:5064–74.

25. Iannone R, Miele L, Maiolino P, Pinto A, Morello S. Blockade of A2b adenosine receptor reduces tumor growth and immune suppression mediated by myeloid-derived suppressor cells in a mouse model of melanoma. Neoplasia 2013;15:1400–9.

26. Wolchok JD, Kluger H, Callahan MK, Postow MA, Rizvi NA, Lesokhin AM, et al. Nivolumab plus ipilimumab in advanced melanoma. N Engl J Med 2013;369:122–33.

27. Curran MA, Montalvo W, Yagita H, Allison JP. PD-1 and CTLA-4 combination blockade expands infiltrating T cells and reduces regulatory T and myeloid cells within B16 melanoma tumors. Proc Natl Acad Sci U S A 2010;107:4275–80.

28. Mangsbo SM, Sandin LC, Anger K, Korman AJ, Loskog A, Totterman TH. Enhanced tumor eradication by combining CTLA-4 or PD-1 blockade with CpG therapy. J Immunother 2010;33:225–35.

29. Duraiswamy J, Kaluza KM, Freeman GJ, Coukos G. Dual blockade of PD-1 and CTLA-4 combined with tumor vaccine effectively restores T-cell rejection function in tumors. Cancer Res 2013;73:3591–603.

30. Ott PA, Hodi FS, Robert C. CTLA-4 and PD-1/PD-L1 blockade: new immunotherapeutic modalities with durable clinical benefit in melanoma patients. Clin Cancer Res 2013;19:5300–9.

31. Guo Z, Wang X, Cheng D, Xia Z, Luan M, Zhang S. PD-1 blockade and OX40 triggering synergistically protects against tumor growth in a murine model of ovarian cancer. PLoS ONE 2014;9:e89350.

32. Wei H, Zhao L, Li W, Fan K, Qian W, Hou S, et al. Combinatorial PD-1 blockade and CD137 activation has therapeutic efficacy in murine cancer models and synergizes with cisplatin. PLoS ONE 2013;8:e84927.

33. Lu L, Xu X, Zhang B, Zhang R, Ji H, Wang X. Combined PD-1 blockade and GITR triggering induce a potent antitumor immunity in murine cancer models and synergizes with chemotherapeutic drugs. J Transl Med 2014; 12:36.

34. Verbrugge I, Hagekyriakou J, Sharp LL, Galli M, West A, McLaughlin NM, et al. Radiotherapy increases the permissiveness of established mammary tumors to rejection by immunomodulatory antibodies. Cancer Res 2012;72:3163–74.

35. John LB, Devaud C, Duong CP, Yong CS, Beavis PA, Haynes NM, et al. Anti-PD-1 antibody therapy potently enhances the eradication of established tumors by gene-modified T cells. Clin Cancer Res 2013;19: 5636–46.

36. Mittal D, Young A, Stannard K, Yong M, Teng MW, Allard B, et al. Antimetastatic effects of blocking PD-1 and the adenosine A2A receptor. Cancer Res 2014;74:3652–8.

37. Cekic C, Linden J. Adenosine A2A receptors intrinsically regulate CD8$^+$ T cells in the tumor microenvironment. Cancer Res 2014;74: 7239–49.

38. Intlekofer AM, Thompson CB. At the bench: preclinical rationale for CTLA-4 and PD-1 blockade as cancer immunotherapy. J Leukoc Biol 2013;94: 25–39.

39. Parry RV, Chemnitz JM, Frauwirth KA, Lanfranco AR, Braunstein I, Kobayashi SV, et al. CTLA-4 and PD-1 receptors inhibit T-cell activation by distinct mechanisms. Mol Cell Biol 2005;25:9543–53.

40. Sheppard KA, Fitz LJ, Lee JM, Benander C, George JA, Wooters J, et al. PD-1 inhibits T-cell receptor induced phosphorylation of the ZAP70/CD3zeta signalosome and downstream signaling to PKCtheta. FEBS Lett 2004; 574:37–41.

41. Yokosuka T, Takamatsu M, Kobayashi-Imanishi W, Hashimoto-Tane A, Azuma M, Saito T. Programmed cell death 1 forms negative costimulatory microclusters that directly inhibit T cell receptor signaling by recruiting phosphatase SHP2. J Exp Med 2012;209:1201–17.

42. Chow CW, Davis RJ. Integration of calcium and cyclic AMP signaling pathways by 14-3-3. Mol Cell Biol 2000;20:702–12.

43. Hermann-Kleiter N, Thuille N, Pfeifhofer C, Gruber T, Schafer M, Zitt C, et al. PKCtheta and PKA are antagonistic partners in the NF-AT transactivation pathway of primary mouse CD3$^+$ T lymphocytes. Blood 2006;107: 4841–8.

44. Takahashi N, Tetsuka T, Uranishi H, Okamoto T. Inhibition of the NF-kappaB transcriptional activity by protein kinase A. Eur J Biochem 2002;269:4559–65.

45. Ramstad C, Sundvold V, Johansen HK, Lea T. cAMP-dependent protein kinase (PKA) inhibits T cell activation by phosphorylating ser-43 of raf-1 in the MAPK/ERK pathway. Cell Signal 2000;12:557–63.

46. Carter L, Fouser LA, Jussif J, Fitz L, Deng B, Wood CR, et al. PD-1:PD-L inhibitory pathway affects both CD4(+) and CD8(+) T cells and is overcome by IL-2. Eur J Immunol 2002;32:634–43.

47. Peng W, Liu C, Xu C, Lou Y, Chen J, Yang Y, et al. PD-1 blockade enhances T-cell migration to tumors by elevating IFN-gamma inducible chemokines. Cancer Res 2012;72:5209–18.

48. Iwai Y, Ishida M, Tanaka Y, Okazaki T, Honjo T, Minato N. Involvement of PD-L1 on tumor cells in the escape from host immune system and tumor immunotherapy by PD-L1 blockade. Proc Natl Acad Sci U S A 2002; 99:12293–7.

49. Blank C, Brown I, Peterson AC, Spiotto M, Iwai Y, Honjo T, et al. PD-L1/B7H-1 inhibits the effector phase of tumor rejection by T cell receptor (TCR) transgenic CD8^{+} T cells. Cancer Res 2004;64: 1140–5.

50. Iannone R, Miele L, Maiolino P, Pinto A, Morello S. Adenosine limits the therapeutic effectiveness of anti-CTLA4 mAb in a mouse melanoma model. Am J Cancer Res 2014;4:172–81.